Reprinted from

NUCLEAR INSTRUMENTS & METHODS IN PHYSICS RESEARCH
Section A

Nuclear Instruments and Methods in Physics Research A 399 (1997) 455–462

Coupling scintillation light into optical fibre for use in a combined PET–MRI scanner

Gerhard M. Haak[a], Nelson L. Christensen[b,*], Bruce E. Hammer[c]

[a] *Department of Electrical and Electronic Engineering, University of Auckland, Auckland, New Zealand*
[b] *Department of Physics, University of Auckland, Private Bag 92019, Auckland, New Zealand*
[c] *Department of Radiology, University of Minnesota, Minneapolis, Minnesota, USA*

Received 15 May 1997; received in revised form 31 July 1997

ELSEVIER

returning to a one-to-one coupling between the scintillation element and photodetector [10,11].

We are currently developing techniques necessary for combining PET and Magnetic Resonance Imaging (MRI) into one scanning device [2,12,13]. This imposes considerable constraints on the architecture of the PET ring that is eventually housed within the MRI bore. The magnetic field adversely affects the functioning of photomultiplier tubes (PMTs), and to protect the homogeneity of the field the metal content of the PET ring must be minimised. A possible solution utilises photodiodes (PD) [8] or avalanche photodiodes (APD) [10] within the magnetic bore; these devices operate in high fields [7, 11], but electrical pick-up of the MRI scanner's pulsed gradient fields would require that PET scans be taken while these gradient fields are off.

The aim of this work is to develop improved methods for carrying the scintillation light away from the source by use of optical fibre, to be detected by a PMT a distance of several metres away [14]. Similar work in coupling scintillation light into optical fibre has been done previously [10,15] but did not explicitly take the angular emission characteristics of the scintillators into account. Calculations and experiments demonstrate that it is possible to guide the scintillation light from a small LSO crystal a distance of several metres without appreciable attenuation, thus opening the possibility for simultaneous registration of MRI and PET data and the additional advantage of increased trans-axial resolution due to the magnetic fields present in MRI.

2. Computer simulations

Crystal simulations were performed with a program using identical physical assumptions to DETECT [16], and has been previously described [17]. Coupling light into an optical fibre where the source has Lambertian emission characteristics, and is butted up against the fibre, is usually estimated from the square of the numerical aperture (NA) of the fibre. This estimate is valid for point sources placed at the centre of the fibre face but does not apply to the crystal. It is instead a surface source defined over the entire face of the fibre, where skew rays become the predominant coupling mode. Skew rays increase the effective NA and the amount of light that is accepted by the fibre; computer simulation is therefore used to estimate the coupling efficiency more accurately. The transmission of the light in the optical fibre is also simulated.

Preceding experimental and simulation studies with BGO have shown the angular light emission characteristics of a parallelipipedal scintillation crystal to be closely approximated by a Lambertian distribution [17]. This places considerable constraints on the methods used to couple the light into optical fibre. It is impossible to concentrate all the light from a Lambertian source into an area that is smaller than the area of the emitter [18]. If the source is smaller than the core of the fibre, optics can be used to image the source such that its dimensions match those of the fibre. However, the coupling efficiency will not exceed the efficiency that would result if the source was as large as the fibre core [19]. It must be noted that the latter calculations assume the NA of the fibre to be small (i.e. the paraxial approximation applies). Using optics will reduce the packing efficiency of the scintillation crystals in the PET scanner, thus adversely affecting the sensitivity and possibly the scanner resolution. Optically coupling the scintillation light into optical fibre should consequently only be considered if strictly necessary.

For the simulations, core-cladding irregularities and mode-coupling are ignored as these typically require many tens of metres to become significant [20]. Coupling and transmission losses due to the curvature of the fibre-cladding surface are calculated using the lossy-ray approximation [21]. Light coupled via the cladding is ignored due to the high attenuation of these transmission modes. Losses due to material imperfections are estimated from the attenuation figures quoted by the manufacturer at the relevant wavelengths.

3. Materials and methods

For the proposed scheme, the fibre must have the following characteristics:

(i) High packing fraction $-C_f \cdot r_1^2/r_2^2$, where r_1 is the core radius, r_2 is the cladding radius, and

C_f is a factor dependent on the method of packing (0.91 for hexagonally packed).

(ii) High numerical aperture to maximise the light capture.

(iii) Low attenuation at the emission wavelength of the scintillator.

(iv) Small individual fibre diameter, to reduce bending losses that will inevitably result when attempting to place a PET ring within the small bore of an MRI machine.

For coupling efficiency and transmission experiments over the 3 m distance, we choose 230 μm diameter 0.49 Na TECT™ [22] hard-clad multimode fibre, which has a core index of 1.46, cladding index of 1.38 and maximum long-term bending radius of 1.3 cm. This favourably compares to a 6.5 cm long-term bending radius for 1000 μm fibre. The packing method is assumed hexagonal, with a packing fraction of 0.91, while the fibre has a core radius of 200 μm, i.e. a core-to-cladding (area) ratio of 0.76. The total (nominal) fractional area covered is therefore 0.91*0.76 = 0.69 (denoted by A_c hereafter). This is approximately the same area fraction one would expect from a single fibre with an identical diameter to the crystal width (crystal cross-section assumed square).

Two square fibre bundles were made, one with dimensions of 2.5 mm × 2.7 mm × 42 cm consisting of 112 fibres, while the other was 2.8 mm × 2.8 mm × 3 m consisting of 176 fibres. In construction, approximately 3 cm of the buffer was mechanically stripped from individual fibres, which were then encased in epoxy resin (Fig. 1), and polished. Optical transmission tests revealed 15 fibres (9%) in the 3 m guide and 12 fibres (11%) in the 46 cm guide were defective (percentage values denoted by η). Because of fabrication errors the guides were not packed to their ideal maximum number of fibres; the 42 cm guide had a 65% filling efficiency while the 3 m guide's was 88%, yielding A_c values for the fibre bundles of 0.46 ± 0.02 and 0.61 ± 0.02 respectively.

A commercially made fibre-bundle light guide (Edmund Scientific, Barrington, NJ) consisting of individual 50 μm fibres of 1 m length and a core refractive index of 1.6 and cladding index of 1.49 (NA of 0.58) is also used for comparison. Because of its size (1 cm diameter) and light attenuation value it is not ideally suited for our PET application, but does provide important information regarding scintillator–fibre bundle coupling.

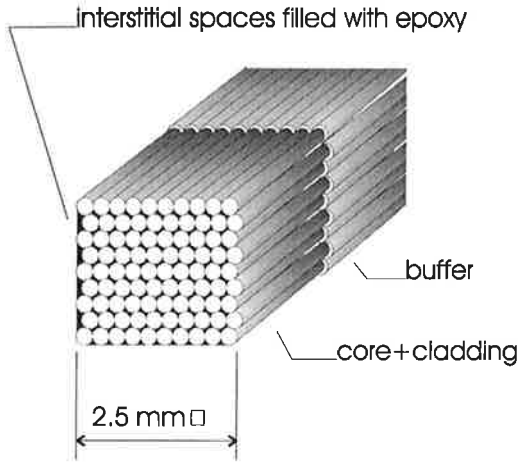

Fig. 1. Fibre–bundle construction. The bundle is the same shape as the crystal. Making the bundle slightly larger than the crystal reduces the effects of misalignment.

A Philips XP2212 PMT (Philips Components, Slatersville, RI) with a radiant photocathode sensitivity of 75 mA/W (21% quantum efficiency) at 420 nm, operates at −1820 V with the lower dynodes linearised at −300 V and is connected to a fast low-noise inverting preamplifier, optionally passing through a 1–13.25 dB attenuator first to prevent signal distortion and/or clipping. The signal is connected to a Nucleus Inc. Model 800 multichannel pulse-height analyser (PHA) with a 1 μs shaping time. The PHA is linked to a PC-compatible computer for data acquisition and analysis (Fig. 2).

LSO is selected as the scintillator of choice, as it has a large conversion efficiency compared to BGO, the traditional PET scintillator. It has a relatively low time constant (50 ns), and lower refractive index (1.82) than BGO (2.15) [23–25]. An LSO crystal of dimensions 2.45 × 2.45 × 10 mm is polished and wrapped in several layers of teflon tape. Glycerol of index 1.47 is used as an optical coupling agent where specified.

4. Experiments and simulations

The LSO crystal is exposed to ^{137}Cs, a 662 keV gamma-ray source, and coupled directly to the

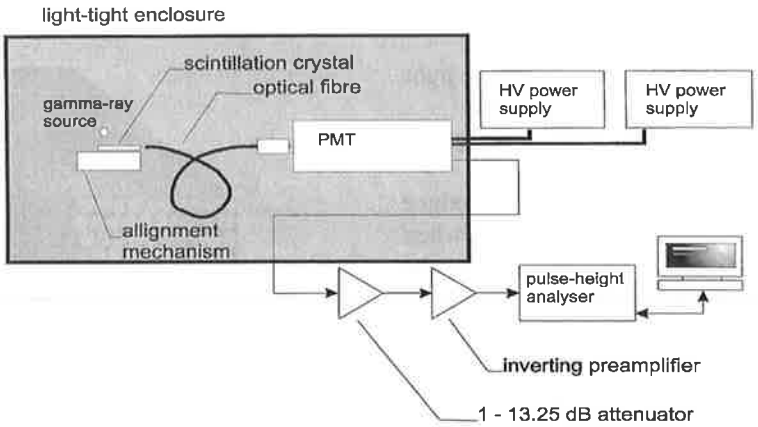

Fig. 2. Experimental set-up for the light-coupling measurements. The attenuator was optional, to allow comparative measurements to be made with accuracy.

PMT. Two data sets are recorded, one with an optical coupling medium between the crystal and PMT, and one without. There is a 50% increase in signal when the coupling agent is used between the crystal and PMT. This allows meaningful comparison of the coupling efficiency for cases where a coupling medium is used between the fibre and crystal.

Coupling efficiency is usually estimated directly from the relative peak positions on the energy spectrums. Illustrated in Fig. 3(A) is the energy spectrum when the 3 m guide is coupled between the crystal and PMT; index matching gel is not used between the crystal–fibre interface, but is present at the fibre–PMT boundary. The spectrum when the LSO crystal is coupled directly to the PMT without an optical coupling agent is shown in Fig. 3(B). It should be noted that the voltage signal is attenuated 13.25 dB for the plot in Fig. 3(B). The peak positions are estimated with a single Gaussian approximation (also shown). The ratio of these two photo-peak signals is (0.173 ± 0.009), and the 662 peak is clearly delineated in both cases. Energy resolutions are 12% for the crystal–PMT coupling, and 30% for the crystal–fibre–PMT coupling. Based on a calibration study of the peak positions and relative energy resolutions, these peaks correspond to approximately 100 and 600 photoelectrons. The photoelectron figures are conservative as the Compton edge contributes to the peak position due to the low energy resolution.

For the fibre-optic coupling simulations with identical conditions, (0.33 ± 0.01) of the light (denoted by P_c) from an area in contact with an individual fibre is coupled and carried to the end of the 3 m fibre. Estimating the attenuation due to fibre imperfections at 100 dB/km (denoted by A_t) [22], the calculated efficiency is

$$\left(10\left(\frac{A_t}{10\,000}\right)\right)^3 (1-\eta) A_c P_c = 0.171 \qquad (1)$$

and compares well with the measured value. The 100 dB/km attenuation factor comes from measurements with scrambled (multi-mode) light [22], and will be approximately valid for skew rays as well. Our simulations indicate that 10% of the light generated by the crystal escapes at the end coupled to the PMT or fibre. Assuming a conversion efficiency of 30 000 photons per MeV [23–25] and 21% PMT quantum efficiency, a 662 keV gamma-ray yields an estimated 420 photoelectrons for a crystal air-coupled to the PMT and approximately 70 photoelectrons with our 3 m fibre bundle. This compares favourably with our measured values. Similar measurements are performed with the 42 cm fibre, but with a ^{22}Na source (Table 1). The ^{22}Na source is not used for

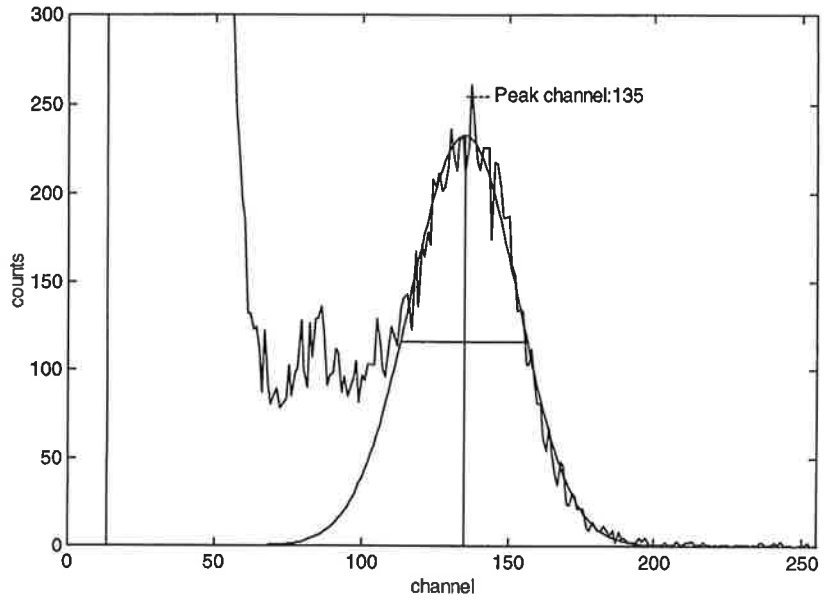

A

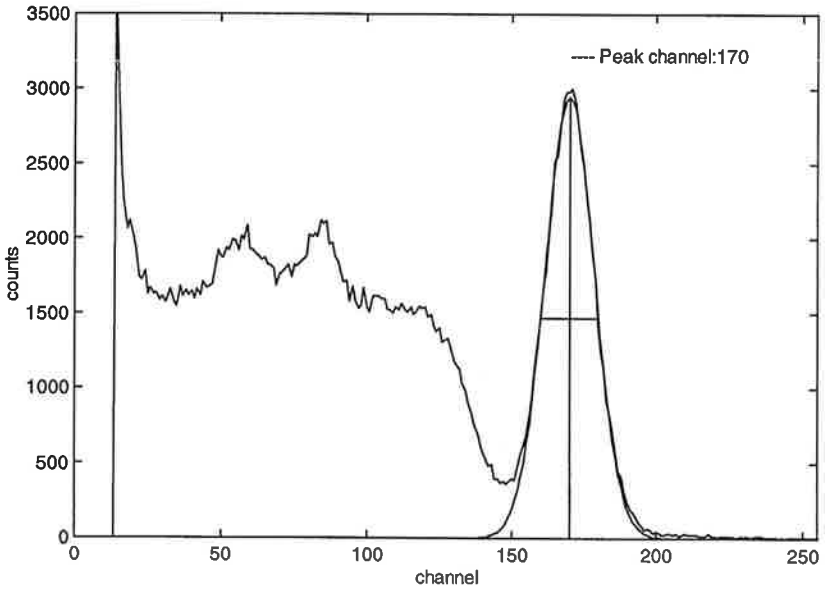

B

Fig. 3. Measured ^{137}Cs energy spectra from the 2.45 mm, 10 mm long, polished LSO crystal wrapped in Teflon tape: (A) With 3 m fibre bundle; (B) LSO crystal only.

Table 1
Measured crystal light output and comparison between measured and calculated coupling efficiencies

Bundle type	Coupling index	Crystal light output (normalized)	Measured coupling and transmission efficiency	Calculated coupling and transmission efficiency	Photo-electons measured	Photo-electrons simulated
42 cm[a]	1.00	0.77	0.111 ± 0.005	0.13	60	40
3 m	1.00	1.00	0.173 ± 0.009	0.17	100	70
1 m	1.00	1.00	0.30 ± 0.01	0.30	180	130
1 m	1.45	1.50	0.186 ± 0.009	0.14	150	90

Note: Crystal light output is normalized to a polished crystal wrapped in Teflon tape, with no optical coupling medium between the crystal and PMT and exposed to a 662 keV source. All calculated coupling efficiencies assume a Labertian source.
[a] Source for the 42 cm fibre is ^{22}Na.

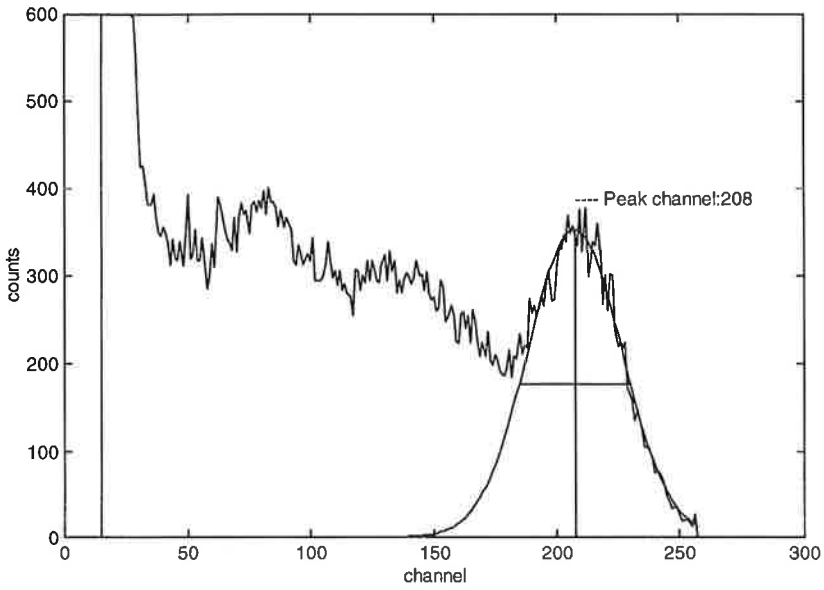

Fig. 4. Measured ^{137}Cs energy spectra from the 2.45 mm, 10 mm long, polished LSO crystal wrapped in Teflon tape and the 1 m commercially manufactured fibre bundle with no optical coupling agent between the crystal and fibre bundle. Of great interest is the fact that the amount of light coupled into the fibre and transmitted to the end is greater than when there is no optical coupling agent present.

the other coupling measurements as it is extremely weak.

The measured efficiency of the 1 m commercial fibre bundle gives a value of (0.30 ± 0.01) for the air-coupled fibre and crystal, equivalent to a signal of 180 photoelectrons, and an energy resolution of 21% (cf. Fig. 4). The fibre-bundle nominally has an area coverage of 0.80 and transmission was specified at 0.76 per meter [26]. Simulations show a P_c factor of (0.49 ± 0.01) over a distance of 1 m for a perfect fibre. Substituting these values into Eq. (1), (assuming $\eta = 0$) gives a calculated total efficiency of 0.30, generating 130 photoelectrons.

Experimentally, there is a 19% reduction in signal through the 1 m fibre when glycerol is used as a coupling agent between the crystal and fibre, compared to the air-interface case (Table 1). For a Lambertian source the fibre-coupling simulations

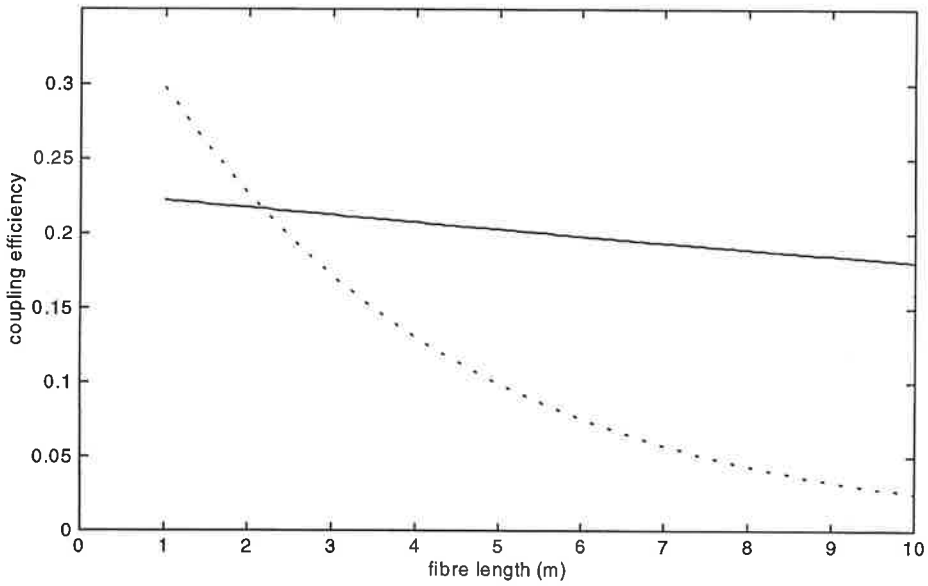

Fig. 5. Calculated total coupling and transmission efficiencies for the 0.58 NA commercial fibre bundle (dashed) and an (ideal) fibre bundle constructed with the lower numerical aperture, 0.49 NA fibre ($A_c = 0.69$, $\eta = 0$, solid line).

indicate a P_c value of only (0.24 ± 0.01) when an optical coupling agent of index 1.45 is used. This may be explained by referring to the effective NA of the fibre, given by [27]

$$\mathrm{NA}_{\mathrm{eff}} = \frac{\sqrt{n_2^2 - n_3^2}}{n_1}, \tag{2}$$

where n_2 is the core index, n_3 is the cladding index and n_1 is the index of the coupling medium. Eq. (2) applies under the assumption that the angular distribution of the light emitted from the source remains unaffected when the index of the coupling medium is non-unity. A value for n_1 greater than unity may affect the light acceptance of the fibre to such an extent as to reduce the absolute amount of light that is guided to the PMT, and shows that the use of index-matching material between the crystals and fibres is an area open for further investigation.

Based on these measurements, it is possible to assess the optimum fibre bundle used to couple the scintillation light over extended distances. Shown in Fig. 5 are the comparative calculated total coupling efficiencies for a 0.58 NA commercial fibre bundle and an ideal fibre bundle constructed with the lower numerical aperture, 0.49 NA fibre ($A_c = 0.69$, $\eta = 0$).

5. Discussion

The development of an efficient and spatially compact means to detect scintillator produced light within the inhospitable environment of an MRI magnet is essential for the development of a dual PET–MRI scanner capable of simultaneous registration of PET and MRI information [2]. Demonstrated in this paper is a technique whereby light from a $2.45 \times 2.45 \times 10$ mm LSO crystal is coupled into a bundle of 176 optical fibres, 3 m long, yielding a measured value of 100 photoelectrons for a 662 keV excitation source with a 30% resolution. The use of small core diameter fibres (200 μm, 0.48 NA) provides the advantage of having reduced bending losses; the allowed long-term bending radius for these fibres is 1.3 cm. This is important as the scintillator light will exit the constrained volume of the MRI magnet bore and travel several meters to photodetectors living in a low magnetic

field region. Larger core light guides, such as those used in other PET applications [10,15] are inappropriate for our concerns, while calculations indicate that high NA fibre, with a corresponding higher attenuation, are also disadvantageous over extended distances. In a PET application (511 keV gamma-ray) our 3 m fibre bundle coupled to a $2.45 \times 2.45 \times 10$ mm LSO crystal will provide 370 scintillator photons at the detector.

Due to the Lambertian emission characteristics of the light from the scintillator [17], it is apparent from work presented by a number of authors [18,19] that the use of optical components will not help in the scintillator–fibre coupling process. In addition, when the fibre is coupled directly to the crystal, the finite extent of the crystal face increases the amount of light coupled into the fibre. The coupling efficiency is greater than what is naively derived from the fibre's NA as skew rays become important. The simulations and experimental measurements also demonstrate that the use of coupling gel at the crystal–fibre interface is inappropriate. Obviously, LSO crystals serve as the best candidate, and the detection of their signal will be straightforward even with relatively inefficient photodetection devices. A BGO signature would be considerably smaller, and hence more challenging to detect. Our fibre bundles could certainly be improved; more efficient packing of the fibres could increase the efficiency by another 10%, while careful preparation will hopefully diminish the damaged fibre value of 9%.

Acknowledgments

This work was supported by grants from the University of Auckland Research Committee, the Auckland Medical Research Foundation, Health Research Council of New Zealand, and the National Institutes of Health (NIH/1R29-CA65523-01A1). We thank Dr. C. Melcher for use of the LSO crystals.

References

[1] M.M. Ter-Pogossian, J. Nucl. Med. 26 (1985) 1487.
[2] R.R. Raylman, B.E. Hammer, N.L. Christensen, IEEE Trans. Nucl. Sci. NS-43 (1996) 2406.
[3] T.F. Bundinger, S.E. Derenzo, R.H. Huseman, W.J. Jaguest, P.E. Valle, Acta. Radiol. 376 (1991) 15.
[4] D.W. Rickey, R. Gordon, W. Huda, Automedica 14 (1992) 355.
[5] H. Iida, I. Kanno, S. Miura, M. Murakami, K. Takahashi, K. Uemura, IEEE Trans. Nucl. Sci. NS-33 (1986) 597.
[6] B.E. Hammer, N.L. Christensen, IEEE Trans. Nucl. Sci. NS-42 (1995) 1371.
[7] B.E. Hammer, N.L. Christensen, B. Heil, Med. Phys. 21 (1994) 1917.
[8] W.W. Moses, S.E. Derenzo, T.F. Budinger, Nucl. Instr. Meth. A 353 (1994) 189.
[9] W.W. Moses, S.E. Derenzo, J. Nucl. Med. 34 (1993) 101.
[10] S.R. Cherry, Y. Shao, M.P. Tornai, S. Siegel, A.R. Ricci, M.E. Phelps, IEEE Trans. Nucl. Sci. NS-42 (1995) 1058.
[11] C. Schmelz, S.M. Bradbury, I. Holl, E. Lorenz, D. Renker, S. Ziegler, IEEE Trans. Nucl. Sci. NS-42 (1995) 1080.
[12] B.E. Hammer, U.S. Patent #4,939,464, 1990.
[13] B.E. Hammer, Physica Medica / Giardini editori e Stampatori, Pisa, Italy. vol. XII Suppl. 1, May 1996; Proc. ESI Seminar: Medical Imaging and New Types of Detectors, Archamps, France, 20–24 May 1995.
[14] N.L. Christensen, B. Hammer, K. Fetterly, B. Heil, Phys. Med. Biol. 42 (1995) 1102.
[15] J.A. McIntyre, R.D. Allen, J. Aguiar, J. T. Paulson, IEEE Trans. Nucl. Sci. NS-42 (1995) 1102.
[16] G.F. Knoll, T.F. Knoll, T.M. Henderson, IEEE Trans. Nucl. Sci. NS- 35 (1988) 872.
[17] G.M. Haak, N.L. Christensen, B.E. Hammer, Nucl. Instr. Meth. A 390 (1997) 191.
[18] T. Jannson, R. Winston, J. Opt. Soc. Am. A 3 (1986) 7.
[19] D. Marcuse, Bell. Syst. Tech. J. 54 (1975) 1507.
[20] J.C. Daly, (Ed.), Fibre Optics, CRC Press, Boca Raton, FL, 1984.
[21] A.W. Snyder, D.J. Mitchell, J. Opt. Soc. Am. 64 (1974) 599.
[22] 3M Technical literature, West Haven, Connecticut, 1996.
[23] C.L. Melcher, J.S. Schweitzer, IEEE Trans. Nucl. Sci. NS-39 (1992) 502.
[24] H. Suzuki, T.A. Tombrello, C.L. Melcher, J.S. Schweitzer, Nucl. Instr and Meth. A 320 (1992).
[25] T. Ludziejewski, K. Moszynska, M. Moszynski, D. Wolfski, W. Klama, L.O. Norlin, E. Devitsin, V. Kozlov, IEEE Trans. Nucl. Sci. NS-42 (1995) 328.
[26] Edmund Scientific Annual Reference Catalog for Optics, Science and Education, 1995.
[27] R. Guenther, Modern Optics, Wiley, Canada, 1990, p. 153.